

Photon Berry phases, Instantons, Quantum chaos and quantum analog of Kolmogorov-Arnold-Moser (KAM) theorem in Dicke models

Yi-Xiang Yu^{1,2,3}, Jinwu Ye^{1,3} and CunLin Zhang³

¹ *Department of Physics and Astronomy, Mississippi State University, P. O. Box 5167, Mississippi State, MS, 39762*

² *School of Instrument Science and Opt-electronics Engineering,
Institute of Optics and Electronics, Beijing University, Beijing 100191, China*

³ *Key Laboratory of Terahertz Optoelectronics, Ministry of Education
and Beijing Advanced innovation Center for Imaging Technology,
Department of Physics, Capital Normal University, Beijing 100048, China*

(Dated: March 8, 2019)

The quantum analog of Lyapunov exponent has been discussed in the Sachdev-Ye-Kitaev (SYK) model and its various generalizations. Here we investigate possible quantum analog of Kolmogorov-Arnold-Moser (KAM) theorem in the $U(1)/Z_2$ Dicke model which contains both the rotating wave (RW) term g and the counter-RW term g' at a finite N . We first study its energy spectrum by the analytical $1/J$ expansion, supplemented by the non-perturbative instanton method. Then we evaluate its energy level statistic (ELS) at a given parity sector by Exact diagonalization (ED) at any $0 < \beta = g'/g < 1$. We establish an intimate relation between the KAM theorem and the evolution of the scattering states and the emergence of bound states as the ratio β increases. We stress the important roles played by the Berry phase and instantons in the establishment of the quantum analogue of the KAM theorem to the $U(1)/Z_2$ Dicke model. Experimental implications in cavity QED systems such as cold atoms inside an optical cavity or superconducting qubits in side a microwave cavity are also discussed.

In classical chaos, the Lyapunov exponent was used to characterize the exponential growth of two classical trajectories when there are just a tiny difference in the initial conditions. The classical concept of Lyapunov exponent can be extended to its quantum analog which can be used to characterize the exponential growth of two initially commuting operators in the early time under the evolution of a quantum chaotic Hamiltonian [1–3]. There are recent flurry of research activities to extract the Lyapunov exponent λ_L on Sachdev-Ye-Kitaev (SYK) models, various variants and its possible dual asymptotic AdS_2 bulk quantum black holes through evaluating Out of time ordered correlation (OTOC) functions [4–15]. From a different perspective, Quantum chaos can also be characterized by the system's energy level statistics (ELS) and level-level correlations encoded in the spectral form factor (SFF) through Random Matrix Theory (RMT)[16, 17]. The ELS and SFF are always evaluated at a finite but sufficiently large system. The ELS of SYK can be described by the Wigner-Dyson (WD) distributions in a $N(\text{mod}8)$ way [16, 17]: $N = 2, 6$ Gaussian unitary ensembles (GUE); $N = 0$ Gaussian orthogonal ensemble (GOE), $N = 4$ Gaussian symplectic ensemble (GSE). The quantum chaos in the SYK models are due to the quenched disorders. However, it inspired a new class of clean models called (colored or un-colored) Tensor (Gurau-Witten) model [18–20] which share similar quantum chaotic properties as the SYK at least in the large N limit.

The quantum chaos in quantum optics also shows up in another class of clean models called Z_2 Dicke models [21]. In the thermodynamic limit $N = \infty$, as the atom-photon coupling strength increases above a criti-

cal value, it displays a normal to a superradiant phase transition. However, the system becomes non-integrable at any finite N . By studying its ELS at a given parity sector by ED at several large finite size $N \geq 10$, the authors [21] found that it is Possionian $P_p(s) = e^{-s}$ in the normal regime, but becomes WD distribution in the GOE $P_w(s) = \frac{\pi}{2}se^{-\frac{\pi}{4}s^2}$ in the superradiant regime. This fact suggests that the onset of the quantum chaos or the changing of ELS through a chaotic to non-chaotic transition (CNCT) may be closely related to the normal to super-radiant phase transition at a finite N . In [26], we studied the $U(1)$ Dicke model [22–25] by a $1/N$ expansion. Obviously, due to the $U(1)$ symmetry, it is integrable and its ELS satisfies Possionian distribution inside the superradiant phase at a finite N . In [31–33], we investigated the $U(1)/Z_2$ Dicke model from both its $U(1)$ limit by a $1/J$ expansion and its Z_2 limit by a strong coupling expansion. The $J - U(1)/Z_2$ Dicke model contains both the rotating wave (RW) term g and the counter-RW term g' at a finite N . It includes the four well known standard quantum optics model in cavity QED such as Rabi [27], Dicke [29], Jaynes-Cummings (JC) [28] and Tavis-Cummings (TC) [30] model as its various special limits. It would be interesting to study the quantum chaos in the $U(1)/Z_2$ Dicke model and its possible connection to the normal to the super-radiant quantum phase transition.

In classical chaos, the classical Kolmogorov-Arnold-Moser (KAM) theorem states that if an integrable Hamiltonian H_0 is disturbed by a small perturbation ΔH , which makes the total Hamiltonian $H = H_0 + \Delta H$, non-integrable. If the two conditions are satisfied: (a) ΔH is sufficiently small (b) the frequencies ω_i of H_0 are incommensurate, then the system remains quasi-integrable.

Just like the quantum analog of Lyapunov exponent can be studied in the context of the SYK models [4–15], it is important to explore the quantum analog of KAM theorem. Despite some previous efforts, the quantum analogue of the KAM theorem remains elusive. In this work, by using the $1/J$ expansion, non-perturbative instanton method, ED and random matrix theory, we explore possible quantum analog of KAM theorem in the $U(1)/Z_2$ Dicke models [37]. These methods are complementary to the strong coupling expansion used by the authors in [33] to study the same model in its dual $Z_2/U(1)$ representation.

Our results are presented in Fig.1-4. When $0 < \beta < \beta_{U(1)} \sim 0.35$, the super-radiant phase at $N = \infty$ splits into the two regimes at a finite N : the $U(1)$ and quantum tunneling (QT) regime [34]. In the $U(1)$ regime, we perform a (non-)degenerate perturbation to evaluate the energy spectrum. It is the Berry phase which leads to the level crossings between the even and odd parity, therefore the alternating parities on the ground state and excited states. In the QT regime, by the WKB method, we find the emergencies of bound states one by one as the interaction strength increases, then investigate a new class of quantum tunneling processes through the instantons between the two bound states in the compact photon phase subject to the Berry phase. It is the Berry phase interference effects in the instanton tunneling event which leads to Schrodinger Cats oscillating with even and odd parities in both ground and higher energy bound states. We also illuminate a duality relation between the eigenenergies in the $U(1)$ regime and those in the QT regime. This duality may be used to explain why the ELS is the same (namely, remains Possionian) in both regimes. However, when $\beta_{U(1)} < \beta \leq 1$, the $U(1)$ regime disappears, so does the duality relation, the system directly crossovers from the normal to the QT regime [34]. Then we study the energy level statistic by ED [21] at a given $0 < \beta < 1$ at a given parity sector. We find that the existence of the $U(1)$ regime when $0 < \beta < \beta_{U(1)}$ implies the validity of the quantum analogue of KAM theorem, therefore the energy level statistics remains Possionian through the whole normal/ $U(1)$ /QT regime. We stress the crucial roles of the Berry phase and instantons in the establishment of the quantum analogue of the KAM theorem to the $J - U(1)/Z_2$ Dicke model. Possible intrinsic connections between the onset of quantum chaos characterized by the RMT and the onset of superradiant phase transition characterized by Renormalization group (RG) are discussed. Experimental implications in detecting quantum chaos in cavity QED systems are also briefly discussed.

RESULTS

1. The $1/J$ expansion in the superradiant phase.

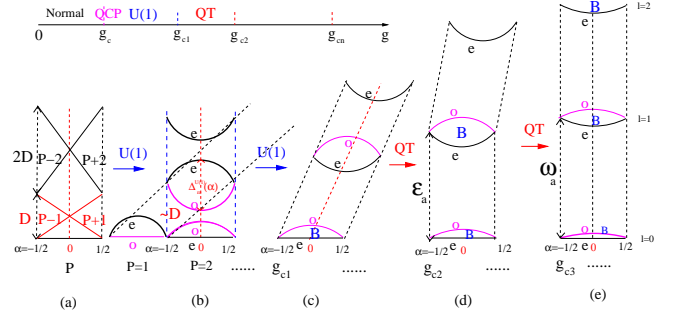


FIG. 1. (Color online) Upper: The superradiant regime at $N = \infty$ splits into the $U(1)$ regime $g_c < g < g_{c1}$ and the QT regime $g > g_{c1}$ at a finite N when $0 < g'/g = \beta < \beta_{U(1)} \sim 0.35$. The quantum critical point (QCP) at $N = \infty$ is at $g_c = \sqrt{\omega_a \omega_b / (1 + \beta)}$. Lower: The atomic energy level evolution from the $U(1)$ regime to the QT regime as g changes at a fixed β near $U(1)$ limit $0 < g'/g = \beta < \beta_{U(1)} \sim 0.35$. The ground state energy has been subtracted. D is the phase diffusion constant. In the $U(1)$ regime in (a) and (b), there are P doublets along the vertical (blue dashed) lines. (a) The energy spectrum at the $U(1)$ limit $\beta = 0$ [31]. (b) The energy level repulsions between the two levels with same parity at $\alpha = 0$. There are also level crossings between the two with opposite parities at $\alpha = \pm 1/2$ in the $U(1)$ regime. All the states are scattering states. If the total excitation P is even, along the vertical (blue dashed) lines, the doublets are organized as $(e, o), (o, e), (e, o), (o, e), \dots$. If P is odd, one need flip all the parities. (c) The doublet at $l = 0$ becomes the first bound state (Schrodinger cat) denoted as B at $g = g_{c1}$, while the states at $l = 1, \dots$ remain scattering states. (d) The doublet at $l = 1$ becomes the second bound state at $g = g_{c2}$, the two bound states at $l = 0, 1$ are connected by nearly straight boundaries at $\alpha = -1/2, 0, 1/2$. The states at $l = 2, \dots$ remain scattering states. (e) Finally, more states become bound states at $g = g_{c3}, \dots$ where the energy level pattern becomes $(e, o), (e, o), \dots$ in the QT regime. If P is odd, one need also flip all the parities. There is a shift by exact one period from (b) to (e). This evolution from (b) to (e) and the fine structures of all the doublets are precisely observed in the ED in Ref.[33]. However, the $U(1)$ regime disappears near the Z_2 limit $\beta_{U(1)} < \beta < 1$. See also Fig.3.

The $J - U(1)/Z_2$ Dicke model[31–33] is described by:

$$H_{U(1)/Z_2} = \omega_a a^\dagger a + \omega_b J_z + \frac{g}{\sqrt{2J}} (a^\dagger J_- + a J_+) + \frac{g'}{\sqrt{2J}} (a^\dagger J_+ + a J_-) \quad (1)$$

where ω_a, ω_b are the energy of the cavity photon and the two atomic levels respectively, $g = \sqrt{N} \tilde{g}, g' = \sqrt{N} \tilde{g}'$; $N = 2J$ are the collective photon-atom rotating wave (RW) coupling and counter-rotating wave (CRW) term respectively. If $\beta = 0$, Eqn.1 reduces to the $U(1)$ Dicke model [22–26, 31] with the $U(1)$ symmetry $a \rightarrow a e^{i\theta}, \sigma^- \rightarrow \sigma^- e^{i\theta}$ leading to the conserved quantity $P = a^\dagger a + J_z$. The CRW g' term breaks the $U(1)$ to the Z_2 symmetry $a \rightarrow -a, \sigma^- \rightarrow -\sigma^-$ with the conserved parity operator $\Pi = e^{i\pi(a^\dagger a + J_z)}$. If $\beta = 1$, it becomes the

Z_2 Dicke model [21, 33]. If $\beta = \infty$, it can be mapped to the static version of Landau-Zener (LZ) model [35]. In this work, we fix the ratio to be $0 < g'/g = \beta < 1$. The other case with $1 < \beta < \infty$ need a different treatment and will be discussed in a separate publication [36, 37].

Following [31], inside the super-radiant phase, it is convenient to write both the photon and atom in the polar coordinates $a = \sqrt{\lambda_a^2 + \delta\rho_a}e^{i\theta_a}$, $b = \sqrt{\lambda_b^2 + \delta\rho_b}e^{i\theta_b}$. When performing the controlled $1/J$ expansion, we keep the terms to the order of $\sim j$, ~ 1 and $\sim 1/j$, but drop orders of $1/j^2$ or higher. We first minimize the ground state energy at the order j and found the saddle point values of λ_a and λ_b :

$$\lambda_a = \frac{g + g'}{\omega_a} \sqrt{\frac{j}{2}(1 - \mu^2)}, \quad \lambda_b = \sqrt{j(1 - \mu)} \quad (2)$$

where $\mu = \omega_a \omega_b / (g + g')^2$. In the superradiant phase $g + g' > g_c^t = \sqrt{\omega_a \omega_b}$. In the normal phase $g + g' < g_c^t$, one gets back to the normal phase $\lambda_a = \lambda_b = 0$. At a fixed β , the QCP happens at

$$g_c = \frac{\sqrt{\omega_a \omega_b}}{1 + \beta} \quad (3)$$

Well inside the superradiant phase, $\lambda_a^2 \sim \lambda_b^2 \sim j$, it is convenient to introduce the \pm modes: $\theta_{\pm} = (\theta_a \pm \theta_b)/2$, $\delta\rho_{\pm} = \delta\rho_a \pm \delta\rho_b$, $\lambda_{\pm}^2 = \lambda_a^2 \pm \lambda_b^2$. The Berry phase in the $+$ sector [26, 31, 32] can be defined as $\lambda_{+}^2 = P + \alpha$ where $P = 1, 2, \dots$ is the closest integer to the λ_{+}^2 , so $-1/2 < \alpha < 1/2$. Due to the large gap in the θ_- sector when $0 < \beta < 1$, it is justified to drop the Berry phase in the $-$ sector. After shifting $\theta_{\pm} \rightarrow \theta_{\pm} + \pi/2$, we reach the Hamiltonian to the order of $1/j$:

$$\mathcal{H}[\delta\rho_{\pm}, \theta_{\pm}] = \frac{D}{2}(\delta\rho_{+} - \alpha)^2 + D_{-}[\delta\rho_{-} + \gamma(\delta\rho_{+} - \alpha)]^2 + 4\omega_a \lambda_a^2 \left[\frac{1}{1 + \beta} \sin^2 \theta_{-} + \frac{\beta}{1 + \beta} \sin^2 \theta_{+} \right] \quad (4)$$

where $D = \frac{2\omega_a(g+g')^2}{E_H^2 N}$ is the phase diffusion constant in the $+$ sector, $D_{-} = E_H^2 / 16\lambda_a^2 \omega_a$ with $E_H^2 = (\omega_a + \omega_b)^2 + 4(g + g')^2 \lambda_a^2 / N$. The $\gamma = \frac{\omega_a^2}{E_H^2} (1 - \frac{(g+g')^4}{\omega_a^4})$ is the coupling between the $+$ and $-$ sector.

When $0 < \beta < 1$, for most purposes, it maybe justified to neglect the quantum fluctuations of the θ_- mode, namely, by setting θ_- at its classical value $\theta_- = 0$, Eqn.4 is simplified to:

$$\mathcal{H}_{+}[\delta\rho_{+}, \theta_{+}] = \frac{D}{2}(\delta\rho_{+} - \alpha)^2 + 2\omega_a \lambda_a^2 \frac{2\beta}{1 + \beta} \sin^2 \theta_{+} \quad (5)$$

Deep inside the superradiant phase $4\lambda_a^2 \frac{\beta}{1 + \beta} \gg 1$ in Fig.1, one can identify the approximate atomic mode:

$$\omega_{-0}^2 = 4\omega_a \lambda_a^2 \frac{2\beta}{1 + \beta} D = \frac{4}{E_H^2} \frac{\beta}{1 + \beta} [(g + g')^4 - g_c^4] \quad (6)$$

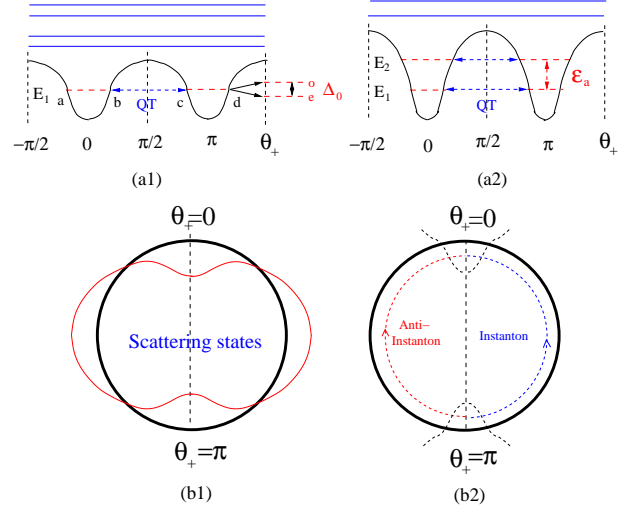


FIG. 2. (Color online) Top: Scattering states, bound states and the quantum tunneling processes in the QT regime. The quantum tunneling splitting Δ_0 and the atomic energy ϵ_a are shown. But the higher optical energy ϵ_o is not shown. (a1) At $g = g_{c1} > g_c$, the double well potential in the θ_+ sector in Eqn.5 holds just one bound state with energy E_1 denoted by a red dashed line. The blue dashed line shows the quantum tunneling between the two bound states which leads to the splitting Δ_0 listed in Eqn.14. The blue solid lines denote scattering states (a2) As the g increases further to $g = g_{c2} > g_{c1}$, the lowest two scattering states in (a1) also become the second bound state with energy $E_2 = E_1 + \epsilon_a$, the third bound state shows up at $g = g_{c3} > g_{c2} > g_{c1}$ and so on (see also Fig.1). The excitation energy is the "atomic" energy ϵ_a . As explained below Eqn.13, the ground state could also be odd parity depending on $(-1)^P$. Bottom: There are qualitative changes in the low lying states in the $U(1)$ and QT regime: (b1) Scattering states in the perturbative $U(1)$ regime: There is a global phase wandering around the θ_+ circle from 0 to 2π with the phase diffusion constant $D \sim 1/N$. (b2) Bound states (Schrodinger cats) in the non-perturbative QT regime: The counterclockwise (blue dashed line) tunneling is an instanton. The clockwise (black dashed line) tunneling is an anti-instanton.

which is the pseudo-Goldstone mode due to the CRW g' term [31, 32].

Note that for sufficiently small $\beta < 1$, the condition to reach the quantum tunneling (QT) regime $4\lambda_a^2 \frac{\beta}{1 + \beta} \gg 1$ is more stringent than the $1/J$ expansion condition $\lambda_a^2 \gg 1$ in the superradiant phase. So there exists a window between the two conditions which is the $U(1)$ regime in Fig.1. This fact will be confirmed by more detailed analysis in the following.

2. $U(1)$ regime and the formation of consecutive bound states in the quantum tunneling (QT) regime. As the potential in the θ_+ sector in Eqn.5 gets deeper and deeper, there are consecutive bound state formations at $g_{c1} < g_{c2} \dots$. The QT regime in Fig.1 is signatored by the first appearance of the bound state at $g = g_{c1}$ after which there are consecutive appear-

ances of more bound states at higher energies leading to the "atomic" energy scale ϵ_a (Fig.2a). The regime $g_c < g < g_{c1}$ is the $U(1)$ regime in Fig.1.

One can estimate all these $g_c < g_{c1} < g_{c2} \dots$ by using the Bohr-Sommerfeld quantization condition for a smooth potential $\int_a^b p d\theta = (n + 1/2)\pi\hbar$, $n = 0, 1, 2, \dots$ where $p = \sqrt{2m(E_{n+1} - V(\theta))}$ and $E_{n+1} = E_1, E_2, \dots$ is the $(n + 1) - th$ bound state energy in Fig.2a. From Eqn.5, we can see that $m = \frac{1}{D}$, $V(\theta) = \omega_a \lambda_a^2 \frac{2\beta}{1+\beta} (1 - \cos 2\theta_+)$ and the a and b are the two end points shown in Fig.2a1. We find that the bound states emerge one by one at

$$\frac{\omega_{-0}}{D} = (n + 1/2) \frac{\pi}{2} \hbar, \quad n = 0, 1, 2, \dots \quad (7)$$

By setting $n = 0$, one can see when $\frac{\omega_{-0}}{D} < \frac{\pi}{4} \hbar$, there is no bound state. This is the $U(1)$ regime in Fig.1. Substituting the expression for the phase diffusion constant D in Eq.4 and the atomic mode ω_{-0} in Eqn.6 leads to the condition for the $U(1)$ regime:

$$4\lambda_a^2 \sqrt{\frac{\beta}{1+\beta}} < \frac{\pi}{4} \quad (8)$$

Note that applying the $1/J$ expansion in the superradiant phase requires $\lambda_a^2 \gg 1$. So for sufficiently small $g'/g = \beta$, there is an appreciable $U(1)$ regime $g_c < g < g_{c1}$ before the quantum tunneling (QT) regime in Fig.1.

The emerging of the bound states one by one after the $U(1)$ regime is shown in Fig.1 and Fig.2. As $g \rightarrow \infty$, $D \rightarrow 0$, while $\omega_{-0} \rightarrow \sqrt{2}\omega_a \sqrt{\frac{2\beta}{1+\beta}}$, so the left hand side of Eqn.7 diverges, there are infinite number of bound states shown in Fig.1e. Obviously, due to the phase wandering in the $U(1)$ regime (Fig.2b1), the Berry phase α in Eqn.5 plays important roles. Naively, the bound state in the QT regime is either localized around $\theta_+ = 0$ or $\theta_+ = \pi$, so the Berry phase plays no roles, so it may be dropped. However, as to be shown in the following sections, it does play very important roles in the quantum tunneling (QT) process due to instantons between the two bound states shown in Fig.2b2.

3. The parity oscillations due to the Berry phase in the $U(1)$ regime. In this $U(1)$ regime, the second term in Eqn.5 breaks the $U(1)$ symmetry to Z_2 symmetry, the Goldstone mode at $N = \infty$ simply becomes the pseudo-Goldstone mode in Eq.6[26, 31, 32]. The total excitation P is not conserved anymore and is replaced by the conserved parity $\Pi = (-1)^P$, the energy levels are only grouped into even and odd parities in Fig.1. One can treat the second term in Eqn.5 perturbatively either by degenerate perturbation expansion at $\alpha = 0$. or a non-degenerate one at $\alpha \neq 0$.

As shown in [31], at a given sector P , there are P crossings at $\alpha = 0$ with $m = 0, \pm 1, \dots, \pm P$. A first order degenerate perturbation [31] at $m = \pm 1$ leads to

the even-odd splitting at $\alpha = 0$ in Fig.1b to be $R_1 = \frac{\omega_a \lambda_a^2}{2} \frac{2\beta}{1+\beta}$. The even-odd gap in the first bubble in Fig.1b is:

$$\Delta_{m=\pm 1, U(1)}(\alpha = 0) = \frac{D}{2} - \frac{\omega_a \lambda_a^2}{2} \frac{2\beta}{1+\beta} \quad (9)$$

which decreases as g increases. Using Eqn.6, one can rewrite $\Delta = \frac{D}{2} [1 - \frac{1}{2}(\frac{\omega_{-0}}{D})^2] > 0$.

For general $\pm m$ (with $|m| \leq P$ in a given sector P), one needs $m - th$ order degenerate perturbation calculation [31] to find the splitting at $\pm m$ to be $R_m \sim (\frac{\omega_a \lambda_a^2}{2} \frac{2\beta}{1+\beta})^m$, $m = 0, 1, \dots, P$, $R_0 = 0$, then $m - th$ even-odd gap at $\alpha = 0$ in the $m - th$ bubble in Fig.1b is:

$$\Delta_{m, U(1)}(\alpha = 0) = D(m + \frac{1}{2}) - R_{m+1} - R_m \quad (10)$$

Setting $m = 0$ recovers Eqn.9.

Note that the degenerate pair $(m, -m - 1)$ at the edge at $\alpha = \pm 1/2$ have opposite parity, so will not be mixed in any order of perturbations [31]. So despite there could be a slight shift in the crossing point between the two opposite parities at $(m, -m - 1)$. the crossing between the pair stays, so

$$\Delta_{m, U(1)}(\alpha = \pm 1/2) = 0 \quad (11)$$

Eq.10 and 11 can be contrasted with Eq.14 and 15 in the QT regime which will be evaluated in the following section.

4. The parity oscillations due to Instantons subject to the Berry phase in the QT regime. At any finite N , there is a QT due to instantons between the two bound states shown in Fig.2 which is a non-perturbative beyond the $1/J$ expansion. The instanton solution for a Sine-Gordon model was well known [38]. From Eqn.5, we can find the classical instanton solution connecting the two minima from $\theta_+ = 0$ or $\theta_+ = \pi$: $\theta_+(\tau) = 2 \tan^{-1} e^{\omega_{-0}(\tau - \tau_0)}$ where τ_0 is the center of the instanton. Its asymptotic form as $\tau \rightarrow \infty$ is $\theta_+(\tau \rightarrow \infty) \rightarrow \pi - 2e^{-\omega_{-0}(\tau - \tau_0)}$. The corresponding classical instanton action is:

$$S_0 = \frac{2\omega_{-0}}{D} \quad (12)$$

The instanton problems in the three well known systems (1) a double well potential (DWP) in a ϕ^4 theory (2) periodic potential problem (PPP) (3) a particle on a circle (POC) are well documented in [38]. The tunneling problem in the present problem is related, but different than all the three systems in the following important ways: (1) the potential $V(\theta) = 2\omega_a \lambda_a^2 \frac{2\beta}{1+\beta} (1 - \cos 2\theta_+)$ in Eqn.5 is a periodic potential in θ_+ . In this regard, it is different than the ϕ^4 theory, but similar to PPP. (2) The θ_+ is a compact angle confined in $0 < \theta_+ < 2\pi$. In this regard, it is different than the PPP, but similar to POC. (3) There are two minima inside the range $0 < \theta_+ < 2\pi$

instead of just one. In this regard, it is different than the POC, but similar to the ϕ^4 theory. (4) Furthermore, it is also important to consider the effects of Berry phase which change the action of instanton to $S_{int} = S_0 + i\alpha\pi$, that of anti-instanton to $\bar{S}_{int} = S_0 - i\alpha\pi$ (Fig.2b2) where $-1/2 < \alpha < 1/2$ is the Berry phase in Eqn.5. So the present quantum tunneling problem is a new class one.

Taking into account the main differences of the present QT problem from the DWP, PPP and POC studied previously [38], especially the crucial effects of the Berry phase, we can evaluate the transition amplitude from $\theta_+ = 0$ to $\theta_+ = \pi$ in Fig.2b2 and also the one from 0 back to 0. The two transition amplitudes lead to the Schrodinger " Cat " state with even/odd parity:

$$\begin{aligned} |e\rangle_{0,SC} &= \frac{A}{\sqrt{2}}(|\theta_+ = 0\rangle + |\theta_+ = \pi\rangle), \\ |o\rangle_{0,SC} &= \frac{A}{\sqrt{2}}(|\theta_+ = 0\rangle - |\theta_+ = \pi\rangle), \end{aligned} \quad (13)$$

where the overlapping coefficient is $A^2 = |\langle x = 0 | n = 0 \rangle|^2 = (\frac{\omega_{-0}}{\pi\hbar D})^{1/2}$. They have the energy $E_{e/o} = \frac{\hbar\omega_{-0}}{2} \mp \Delta_0/2$ with the splitting between them given by:

$$\begin{aligned} \Delta_0(\alpha) &= 8\omega_{-0}(\cos \alpha\pi)\left(\frac{\omega_{-0}}{\pi D}\right)^{1/2}e^{-\frac{2\omega_{-0}}{D}} \\ &\sim (\cos \alpha\pi)\sqrt{N}e^{-cN} \end{aligned} \quad (14)$$

which decreases as g increases.

One can see that it is the Berry phase which leads to the oscillation of the gap and the parity of the ground state. It vanishes at the two end points $\alpha = \pm 1/2$ and reaches maximin at the middle $\alpha = 0$. Note that the Berry phase α is defined [26, 31, 32] at a given sector P . So Eqn.13 has a background parity $\Pi = (-1)^P$. So there is an infinite number of oscillating parities in Eqn.13 as g increases.

Because the Berry phase effects remain in the given P sector, extending the results in Ref.[39], we find the splitting in the n -th excited bound states ($n = 0, 1$ in Fig.2a2):

$$\Delta_n(\alpha) = \frac{1}{n!}\left(\frac{8\omega_{-0}}{D}\right)^n \Delta_0 \quad (15)$$

where $n = 0, 1, 2, \dots$ with the corresponding n -the Schrodinger "Cat" state with even/odd parity and the energy $E_{e/o,n} = (n + \frac{1}{2})\hbar\omega_{-0} \mp \Delta_n/2$. Eq.14 in the QT regime can be contrasted with Eq.10 and 11 in the $U(1)$ regime.

One can see the higher the bound state in the Fig.2, the larger the splitting is. These results are completely consistent with those achieved from the strong coupling expansion in [33] after identifying $n \sim l$. For example, there is an extra oscillating sign $(-1)^l$ in Eqn.5 in [33] achieved from the strong coupling expansion, which is crucial to reconcile the results achieved from the two independent approaches !

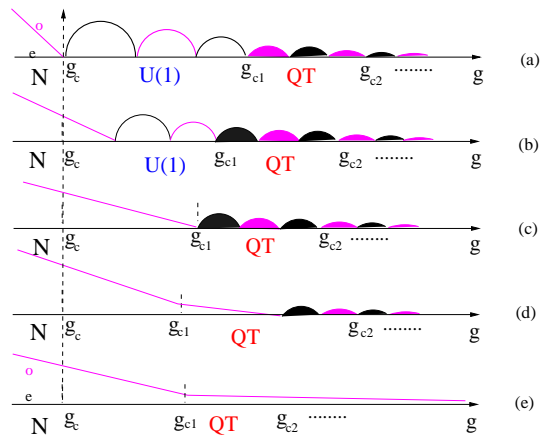


FIG. 3. (Color online) The evolution of the two lowest energy with even and odd parity. (a) is the same as the two lowest states in Fig.1. (a) and (b) where $0 < \beta < \beta_{U(1)} \sim 0.35$, the first oscillation happens before the first formation of the bound state at g_{c1} . In the normal regime, there is no oscillations. In the $U(1)$ regime before g_{c1} , the oscillations are due to the scattering states (open bubbles). In the QT regime after g_{c1} , the oscillations are due to the bound states (shaded bubbles). The ELS stays Possionain, there is no CNCT as g increases. As β increases, the $U(1)$ regime shrinks from (a) to (b). (c) where $\beta = \beta_{U(1)} \sim 0.35$, the first oscillation happens at the same time as the formation of the bound state at g_{c1} . The $U(1)$ regime just disappears. (d) and (e) where $\beta_{U(1)} < \beta \leq 1$, it happens after the first formation of the bound state at g_{c1} . The $U(1)$ regime does not exist anymore. When $\beta = 1$, the oscillation was pushed to infinity, so there is no oscillations at all after the formation of the bound states. There is a CNCT near g_c where the ELS changes from the Possionain to GOE. Compare to Fig.4.

The $U(1)$ regime and the QT regime can be theoretically well distinguished by its qualitatively different features (Fig.3): When $0 < \beta < \beta_{U(1)}$, the even-odd oscillations happen *before* the formation of the bound states (Fig.3a,b), so there are two regimes: the $U(1)$ (perturbative) regime where the maximum gap at $\alpha = 0$ Eq.10 get reduced $< D(m + 1/2) \sim 1/N$ as g increases and the QT (non-perturbative) regime where the maximum gap at $\alpha = 0$ Eq.14 scales as $\sqrt{N}e^{-N}$ and also reduces as g increases. However, when $\beta_{U(1)} < \beta < \infty$, the even-odd oscillations happen *after* the formation of the bound state (Fig.3d,e), the $U(1)$ regimes does not exist anymore, the system directly crossover from the normal regime to the QT regime. Of course, at $\beta = \beta_{U(1)}$, the oscillations start with the formation of the bound state (Fig.3c). Unfortunately, practically, it is numerically challenging to determine the precise value of $\beta_{U(1)}$ at any finite N . However, it was estimated by ED in [31] to be $\beta_{U(1)} \sim 1/3$. The important phenomena of Goldstone and Higgs mode at the $U(1)$ limit $\beta = 0$ can still be observed in this $U(1)$ regime.

5. The energy level statistics and the chaotic to non-chaotic transitions (CNCT). Here we study

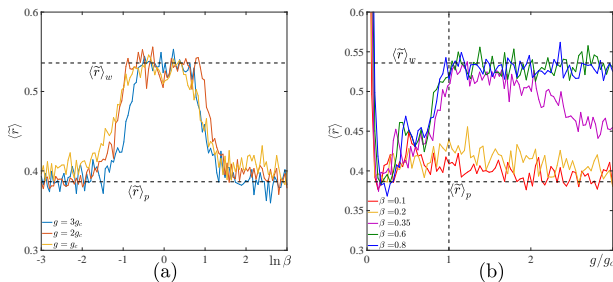


FIG. 4. (Color online) The mean values of the ratio \tilde{r} at $N = 20$ (a) versus $\ln \beta$ at the resonant case $\omega_a = \omega_b$ in the superradiant phase at different $g/g_c = 3, 2, 1$. The analytical mean values of \tilde{r} in PD and WD are marked as references. There is a CNCT tuned by β near $\beta \sim 0.37$ when $g/g_c \geq 1$. This value [42] seems also insensitive to the value g/g_c as long as it is at the QCP or inside the superradiant phase $g/g_c \geq 1$. (b) versus g/g_c at 5 different $\beta = 0.1, 0.2, 0.35, 0.6, 0.8$ corresponding to Fig.3a-e. There is a CNCT tuned by g/g_c near $g/g_c = 1$ when $\beta_{U(1)} < \beta < 1$, but no such a transition when $0 < \beta < \beta_{U(1)}$. In both cases, when $g/g_c < 0.15$, \tilde{r} shoots up to 1, the system just tends to be regular instead of being random [43]. When $g/g_c \rightarrow \infty$, there are infinite number of bound states in Fig.1 which push out all the scattering states, so it becomes regular too instead of being random.

the energy level statistics at a given $0 < \beta < 1$. One can define the anti-unitary Time reversal symmetry $\mathcal{T} = K$ which takes complex conjugate on the atomic spin operators (See footnote Ref.31 in [33]). Obviously, $\mathcal{T}^2 = 1$, so just from symmetry point of view, it is in GOE. Practically, one need to perform a specific ED to test if a specific Hamiltonian indeed satisfies GOE. If the KAM theorem applies is out of the symmetry classification and can only be tested by specific calculations.

At the $U(1)$ limit $g' = 0$ ($\beta = 0$), the Dicke model is integrable. So the energy level always satisfies the Poisson distribution $P_p(s) = e^{-s}$. At the Z_2 limit $\beta = 1$, the system becomes non-integrable at any finite N , the energy level statistics (ELS) is Possionian in the normal regime, but becomes Wigner-Dyson (WD) distribution in the Grand orthogonal ensemble (GOE) $P_w(s) = \frac{\pi}{2} s e^{-\frac{\pi}{4} s^2}$ in the superradiant regime [21]. This fact suggests that the emergence of the quantum chaos or the changing of ELS thorough a CNCT at any finite N may be related to the normal to super-radiant phase transition. Now we will study the energy level statistic by ED [21] at a given $0 < \beta < 1$ at a given parity sector, then compare with the analytical results on the low energy level evolution from the normal, $U(1)$ regime to the QT regime in Fig. 1 and Fig.3 to explore their possible intrinsic connections.

The nearest-neighbor energy level spacings $s_n = E_n - E_{n-1}$ where we labeled all the energy levels in the descending orders $E_0 < E_1 < E_2 < \dots < E_n < \dots$. By ED, we drew the diagram of s_n versus n for tunable

cutoff from $n = 400$ to $n = 4000$ at various $\beta = 1, 0.8, 0.5, 0.2, 0.1$. After determining the optimal energy level spacing ds which can distinguish the two level spacing most efficiently, we also evaluated the energy level statistics $P(s)$ on $s = s_n/\bar{s}$ where \bar{s} is the mean value of $\{s_n\}$ at these β values [41].

To get rid of the dependence on the local density of states, it is convenient to look at the distribution of the ratio of two adjacent energy level spacings [16, 40] $r_n = \frac{s_n}{s_{n+1}}$ which distributes around 1. Then $P_p(s)$ and $P_w(s)$ leads to $p_p(r) = \frac{1}{(1+r)^2}$ and $p_w(r) = \frac{1}{Z} \frac{(r+r^2)^\beta}{(1+r+r^2)^{1+3\beta/2}}$, $\beta = 1, Z = 8/27$ respectively. We computed the distribution of the logarithmic ratio [16, 40] $P(\ln r) = p(r)r$. Because $p(\ln r) dr$ is symmetric under $r \leftrightarrow 1/r$, one may confine $0 < r < 1$ and double the possibility density $p(\tilde{r}) = 2p(r)$. Therefore, the above two distributions have two different expected values of $\tilde{r} = \min\{r, 1/r\}$:

$$\begin{aligned} \langle \tilde{r} \rangle_p &= \int_0^1 2p_p(r) dr = 2 \ln 2 - 1, \\ \langle \tilde{r} \rangle_w &= \int_0^1 2p_w(\beta = 1, r) dr = 4 - 2\sqrt{3} \end{aligned} \quad (16)$$

We plot $\langle \tilde{r} \rangle$ vs $\ln \beta$ in Fig.4a at a fixed $g/g_c = 3, 2, 1$ which is at the QCP (namely, along the dashed line in Fig.3) or inside the superradiant phase. It shows that there is a CNCT at $\ln \beta \sim \pm 1$, so the CNCT tuned by β happens near $\beta \sim 0.37$. As shown in Fig.4b, there is a CNCT near $g/g_c = 1$ tuned by g at a fixed $\beta_{U(1)} < \beta < 1$ but none when $0 < \beta < \beta_{U(1)}$.

6. The Berry phase effects lead to the quantum analogue of the Kolmogorov-Arnold-Moser (KAM) theorem. Here we explore a possible quantum analogue of the classical KAM theorem in the context of $J - U(1)/Z_2$ Dicke model. The $U(1)$ Dicke model at $\beta = 0$ is integrable. If ignoring the Berry phase α , its eigen-energy would be commensurate. So it is the frustration due to the Berry phase effects which make its eigen-energies become in-commensurate [26, 31] except at $\alpha = 0, \pm 1/2$ which have zero measures anyway, so the quantum analogue of the KAM theorem may apply.

As shown in Fig.4b, at a given β , if there is one (in fact, only one) CNCT tuned by g/g_c , it happens near the QCP $g/g_c = 1$. So one may just focus on how the ELS changes at $g/g_c = 1$ as β decreases (along the dashed line in Fig.3). The ELS in (e) must be GOE, remains GOE in (d), must be Possionian in (a) and remain to be Possionian in (b), so the CNCT must happen at $\beta = \beta_{U(1)}$ where the $U(1)$ regime just disappears in (c).

We make the following statement on the quantum analogue of the KAM theorem (1) *The existence of the $U(1)$ regime between the normal phase and the QT regime when $0 < \beta < \beta_{U(1)}$ indicates that the quantum KAM theorem apply, the ELS remains Possionian throughout*

the normal, $U(1)$ and the QT regime. In fact, as shown below, there is a duality relation between the eigenenergies in the $U(1)$ regime and those in the QT regime. (2) The absence of the $U(1)$ regime when $\beta_{U(1)} < \beta < 1$ indicates that the quantum KAM theorem fails, the ELS changes from Possionian in the normal to Wigner-Dyson in the QT regime. Of course, the duality relation also disappears. This conclusion is expected to also hold when $1 < \beta < \infty$ when one moves from the Z_2 limit at $\beta = 1$ to the LZ limit [36] at $\beta = \infty$. This conclusion is in sharp contrast to the claims made in [37]. The main reason is that Ref.[37] is a purely numerical data without any physical insights from analytical calculations.

The ELS in Fig.1 (see also Fig.3a,b) must be Possionian. The bound states will appear one by one in the QT regime in Fig.1c-e. However, because their numbers are finite anyway, so will not affect the ELS which involves infinite number of energy levels. So the ELS stays Possionian from the $U(1)$ to the QT regime in Fig.1.

In fact, there are some illuminating duality in the quantum numbers characterizing the energy spectrum when $0 < \beta < \beta_{U(1)}$. In the $U(1)$ regime in Fig.1 and 3a,b, it is convenient to use the complete eigenstates $|l\rangle_m|m\rangle$ where the Landau level index $l = 0, 1, \dots, N$ ($N+1$ Landau levels) denotes the high energy Higgs type of excitation, the magnetic number $m = -P, -P+1, \dots$ (no upper bounds) denotes the low energy pseudo-Goldstone mode [31]. In the QT regime in Fig.1 and 3a,b, it is convenient to use a different set of complete eigenstates $|l\rangle_m|j, m\rangle$ where the Landau level index $l = 0, 1, \dots$ (no upper bounds) denotes the low energy atomic excitation, the magnetic number $m = -j, -j+1, \dots, j$ (also $2j+1 = N+1$) denotes the high energy optical mode [33]. So the Landau level index and the magnetic number exchanges their roles from the $U(1)$ to the QT regime when $0 < \beta < \beta_{U(1)}$. This duality relation between the two sets of eigenstates implies that the ELS remains the same from the $U(1)$ to the QT regime, namely, remains to be Possionian. Of course, when $\beta_{U(1)} < \beta < 1$, the $U(1)$ regime disappears and so does the duality relations.

One may also understand the quantum analog of the KAM theorem from a dual point of view, namely from the chaotic Z_2 limit and investigate how the chaotic behaviours change to non-chaotic as a perturbation acts on. At $\beta = 1$, the super-radiant phase becomes the QT regime at any finite N (Fig.3e). As g decreases, the CNCT transition happens near $g/g_c = 1$. When not too far away from the Z_2 limit $\beta_{U(1)} < \beta < 1$, the super-radiant phase still becomes the QT regime at any finite N (Fig.3d). As g decreases, the CNCT transition still happens at $g/g_c = 1$. However, when β decreases to $0 < \beta < \beta_{U(1)}$ (Fig.3a,b), the super-radiant phase splits into the QT regime and the $U(1)$ regime. The CNCT disappears, the ELS remains Possionian.

DISCUSSIONS.

In this work, we only focused on the the ELS of the

bulk spectrum. In fact, when doing the ELS, one can even just throw away the low energy bound states which are finite number anyway. So the bulk states simply reflect the high energy scattering states. It would be interesting to just focus on the edge spectrum which can reflect the low energy bound states. So in a future publication, we may study the ELS of the edge spectrum to reflect the bound state evolution in Fig.3.

As said in the introduction, in addition to the ELS in the RMT classifications, the CNCT may also be diagnosed from the spectral form factor (SFF) in the RMT. The SFF at $\beta_T = 0$ may also be a useful diagnostic tool for the CNCT. A slope-dip-ramp-plateau structure was considered to be evidence for quantum chaotic behaviours. This feature may disappear when $0 < \beta < \beta_{U(1)}$. While the Lyapunov exponent at an early time is a completely different way to characterize the quantum chaos. So it may also be interesting to investigate the KAM from the OTOC perspective. For the $U(1)/Z_2$ Dicke models, fixing at a given $g/g_c \geq 1$ (at the QCP or the superradiant phase in Fig.3 and Fig.4a), we expect that the Lyapunov exponent λ_L at the infinite temperature $\beta_T = 0$ reaches maximum at the Z_2 limit $\beta = 1$, then decreases as β becomes smaller than 1, becomes zero at $\beta_{U(1)}$, remains to be zero when $0 < \beta < \beta_{U(1)}$. These results will be presented in a separate publication [36].

The Quantum analog of KAM theorem at a generic $0 < \beta < 1$ in the $U(1)/Z_2$ Dicke model may be contrasted with the QPT from the normal to the super-radiant phase. In the $U(1)/Z_2$ Dicke model, any $g' > 0$ breaks explicitly the $U(1)$ symmetry of the integrable $U(1)$ Dicke model and is clearly a relevant perturbation. There is a line of fixed point at $g_c = \frac{\sqrt{\omega_a \omega_b}}{1+\beta}$ tuning from the $U(1)$ limit at $\beta = 0$ to the Z_2 limit at $\beta = 1$. QPT only involves the changing of the ground states and the low energy excitations, while the high energy states are irrelevant. Strictly speaking, it happens only in the thermodynamic limit $N \rightarrow \infty$ when symmetry broken can happen, there is no QPT in any finite systems. While the ELS in RMT involves all the energy levels at a finite but large enough N . In a recent preprint [46], we studied quantum chaos and quantum analog of Kolmogorov-Arnold-Moser (KAM) theorem in hybrid Sachdev-Ye-Kitaev (SYK) models and contrasted with those in the $U(1)/Z_2$ Dicke model studied in this paper. We found that the similar phenomena also appear in the hybrid SYK models [46]. So despite the absence of QPT in the present cases of the $U(1)/Z_2$ Dicke model and hybrid SYK models, there could still be a CNCT.

It was well established that in terms of symmetries and the space dimension, the Renormalization Group (RG) (including the DMRG, MPS and tensor network) can be used to classify many body phases and phase transitions [44, 45]. The RG focus on either infra-red (IR) behaviours of the system which are determined by the

ground state and low energy excitations. The RG is also intimately connected to General Relativity (GR) through the holographic principle. The 10-fold way in RMT can be classified just by a few global discrete symmetries. It covers all the energy levels of the system in the Hilbert space and can also be used to characterize the CNCT. Possible deep connections between the onset of quantum chaos characterized by the RMT and the onset of quantum phase transition characterized by the RG need to be explored further. The $U(1)/Z_2$ Dicke models and the hybrid SYK models (or the GW tensor models) may supply new platforms to investigate possible relations between the two dramatically different classification schemes.

Finally, we comment on the experimental realizations of the $U(1)/Z_2$ Dicke model. Due to recent tremendous advances in technologies, the $U(1)/Z_2$ Dicke model has been realized in at least two kinds of cavity QED systems (1) a BEC atoms inside an ultrahigh-finesse optical cavity [47–51] and (2) superconducting qubits inside a microwave circuit cavity [52–55] or quantum dots inside a semi-conductor microcavity [56]. All the results achieved in this work should be detected in these systems by various standard quantum optics techniques such as fluorescence spectrum, phase sensitive homodyne detection and Hanbury-Brown-Twiss (HBT) type of experiments respectively [57–59]. Our work shows that the cavity QED systems may provide experimentally accessible systems to investigate quantum chaos and quantum information scramblings in strong light-matter interacting systems.

Acknowledgements

JY acknowledges AFOSR FA9550-16-1-0412 for supports. CLZ's work has been supported by National Keystone Basic Research Program (973 Program) under Grant No. 2007CB310408, No. 2006CB302901 and by the Funding Project for Academic Human Resources Development in Institutions of Higher Learning Under the Jurisdiction of Beijing Municipality.

[1] A. I. Larkin and Y. N. Ovchinnikov, "Quasi-classical method in the theory of superconductivity ", JETP 28, 6 (1969); 1200-1205

[2] S. H. Shenker and D. Stanford, Black holes and the butterfly effect," JHEP 03, 067 (2014), arXiv:1306.0622 [hep-th].

[3] J. Maldacena, S. H. Shenker, and D. Stanford, A bound on chaos," ArXiv e-prints (2015), arXiv:1503.01409 [hep-th].

[4] S. Sachdev and J. Ye, Gapless spin liquid ground state in a random quantum Heisenberg magnet," Phys. Rev. Lett. 70, 3339 (1993), cond-mat/9212030.

[5] A. Georges, O. Parcollet, and S. Sachdev, Quantum fluctuations of a nearly critical Heisenberg spin glass," Phys. Rev. B 63, 134406 (2001), cond-mat/0009388.

[6] A. Y. Kitaev, Talks at KITP, University of California, Santa Barbara," Entanglement in Strongly- Correlated Quantum Matter (2015).

[7] S. Sachdev, Bekenstein-Hawking Entropy and Strange Metals," Phys. Rev. X 5, 041025 (2015), arXiv:1506.05111 [hep-th].

[8] J. Polchinski and V. Rosenhaus, The Spectrum in the Sachdev-Ye-Kitaev Model," JHEP 04, 001 (2016), arXiv:1601.06768 [hep-th].

[9] J. Maldacena and D. Stanford, Remarks on the Sachdev-Ye-Kitaev model," Phys. Rev. D 94, 106002 (2016), arXiv:1604.07818 [hep-th].

[10] W. Fu and S. Sachdev, Numerical study of fermion and boson models with infinite-range random interactions," Phys. Rev. B 94, 035135 (2016), arXiv:1603.05246 [cond-mat.str-el].

[11] D. J. Gross and V. Rosenhaus, A Generalization of Sachdev-Ye-Kitaev," (2016), arXiv:1610.01569 [hep-th].

[12] D. Bagrets, A. Altland, and A. Kamenev, Sachdev-Ye-Kitaev model as Liouville quantum mechanics," Nucl. Phys. B 911, 191 (2016), arXiv:1607.00694 [cond-mat.str-el]. It was shown in this work and [14] that the Lyapunov exponent $\lambda_L = 0$ at even lower temperature $k_B T < J/N$ for $q = 4$ SYK.

[13] J. Maldacena, D. Stanford, and Z. Yang, Conformal symmetry and its breaking in two dimensional Nearly Anti-de-Sitter space," (2016), arXiv:1606.01857 [hep-th].

[14] Thomas G. Mertens, Gustavo J. Turiaci, Herman L. Verlinde, Solving the Schwarzian via the Conformal Bootstrap, arXiv:1705.08408.

[15] Douglas Stanford, Edward Witten, Fermionic Localization of the Schwarzian Theory, arXiv:1703.04612.

[16] Y.-Z. You, A. W. W. Ludwig, and C. Xu, Sachdev-Ye-Kitaev Model and Thermalization on the Boundary of Many-Body Localized Fermionic Symmetry Protected Topological States," ArXiv eprints (2016), arXiv:1602.06964 [cond-mat.str-el]. Phys. Rev. B 95, 115150 (2017)

[17] J. S. Cotler, G. Gur-Ari, M. Hanada, J. Polchinski, P. Saad, S. H. Shenker, D. Stanford, A. Streicher, and M. Tezuka, Black Holes and Random Matrices," (2016), arXiv:1611.04650 [hep-th].

[18] Razvan Gurau, The complete $1/N$ expansion of a SYK-like tensor model, arXiv:1611.04032

[19] Edward Witten, An SYK-Like Model Without Disorder, arXiv:1610.09758 [hep-th]

[20] Igor R. Klebanov, Grigory Tarnopolsky, Uncolored Random Tensors, Melon Diagrams, and the SYK Models, Phys. Rev. D 95, 046004 (2017), arXiv:1611.08915 [hep-th].

[21] C. Emary and T. Brandes, Phys. Rev. Lett. 90, 044101 (2003); Phys. Rev. E 67, 066203 (2003). It was shown that only when $N \geq 6$, it make sense to talk about the ELS. For example, the $N = 1$ case which is the Rabi model, it makes no sense to study its ELS.

[22] K. Hepp and E. H. Lieb, Anns. Phys. (N. Y.), 76, 360 (1973); Y. K. Wang and F. T. Hioe, Phys. Rev. A, 7, 831 (1973).

[23] V. N. Popov and S. A. Fedotov, Soviet Physics JETP, 67, 535 (1988); V. N. Popov and V. S. Yarumin, Collective Effects in Quantum Statistics of Radiation and Matter (Kluwer Academic, Dordrecht,1988).

[24] P. R. Eastham and P. B. Littlewood, Phys. Rev. B 64, 235101 (2001).

- [25] V. Buzek, M. Orszag and M. Roko, Phys. Rev. Lett. 94, 163601 (2005).
- [26] Jinwu Ye and CunLin Zhang, Super-radiance, Photon condensation and its phase diffusion, Phys. Rev. A 84, 023840 (2011).
- [27] I.I. Rabi, Phys. Rev. 49, 324 (1936); 51, 652 (1937).
- [28] E. T. Jaynes and F. W. Cummings, Proc. IEEE 51, 89 (1963).
- [29] R.H. Dicke, Phys. Rev. 93, 99 (1954)
- [30] M. Tavis and F.W. Cummings, 170, 379 (1968).
- [31] Yu Yi-Xiang, Jinwu Ye and W.M. Liu, Scientific Reports 3, 3476 (2013).
- [32] Yu Yi-Xiang, Jinwu Ye, W.M. Liu and CunLin Zhang, arXiv:1506.06382.
- [33] Yu Yi-Xiang, Jinwu Ye and CunLin Zhang, Parity oscillations and photon correlation functions in the $Z_2/U(1)$ Dicke model at a finite number of atoms or qubits, Physical Review A 94.2 (2016), 023830.
- [34] In this paper, at a finite N , we use the superradiant phase to stand for the combination of the $U(1)$ regime and the QT regime when the $U(1)$ regime exists at $0 < \beta < \beta_{U(1)}$. When $\beta_{U(1)} < \beta < 1$, because the $U(1)$ regime disappears, it just stands for the QT regime.
- [35] Alexander Altland, V. Gurarie, T. Kriecherbauer, and A. Polkovnikov, Nonadiabaticity and large fluctuations in a many-particle Landau-Zener problem, Phys. Rev. A 79, 042703 C Published 2 April 2009.
- [36] Yu Yi-Xiang, *et.al*, unpublished.
- [37] There is a purely numerical work to discuss the CNCT in the $U(1)/Z_2$ Dicke model. Wouter Buijsman, Vladimir Gritsev, and Rudolf Sprik, Nonergodicity in the Anisotropic Dicke Model, Phys. Rev. Lett. 118, 080601 C Published 23 February 2017. Furthermore, this paper also made a mistake to identify the $0 < \beta < 1$ case with the $1 < \beta < \infty$ case. As shown below Eq.1, if $g = 0$, it can be mapped to the static version of Landau-Zener (LZ) model [35]. In this work, we fix the ratio to be $0 < g'/g = \beta < 1$. The other case with $1 < \beta < \infty$ need a completely different treatment and will be discussed in a separate publication [36]. See also [42].
- [38] S. Coleman, Aspects of Symmetry, Cambridge University Press, 1985, A. M. Polyakov, Gauge Fields and Strings, Harwood Academic Publishers, 1987; R. Rajaraman, Solitons and Instantons, North-Holland Publishing Company, 1982
- [39] U. Weiss and W. Haffner, Phys. Rev. D 27, 2916 (1983).
- [40] Y. Y. Atas, et al. "Distribution of the ratio of consecutive level spacings in random matrix ensembles." Physical review letters 110.8 (2013): 084101.
- [41] The way we collect the ELS of the $U(1)$ Dicke model need a special note. The $U(1)$ Dicke model $g' = 0$ in Eq.1 has a conserved quantity $P = a^\dagger a + J_z + J$. When $P < N$ (or $P > N$), there are $P + 1$ (or $N + 1$) state [31].
- So when collecting the ESL of the $U(1)$ Dicke model, we take all the energy levels at all possible different P which fit the Poissonian distribution. If confining to a fixed P sub-Hilbert space, we can not get any sensible ELS. This is in contrast to the way in [16] to collect the ELS of complex SYK at a given $Q = \sum_i c_i^\dagger c_i$, also the way at the hybrid SYK models to be presented in [46]. Of course, any $g' \neq 0$ in Eq.1 breaks the $U(1)$ symmetry, only the parity $\Pi = e^{i\pi Q}$ becomes a conserved quantity. So we collect the ELS at a given parity sector. For all the cases from the $U(1)$ to the Z_2 limit, there is always a regular regime when $g/g_c < 0.15$.
- [42] It seems Fig.4 enjoys a emergent symmetry $\beta \leftrightarrow 1/\beta$. This possible emergent symmetry in ELS will be explored from both the $U(1)$ Dicke model side $0 < \beta < 1$ and the Landau-Zener model side $1 < \beta < \infty$ in Ref.[36].
- [43] Being regular means the energy levels show a regular behaviours, so the ELS satisfies neither Poisson nor WD. Being random means the energy levels show random distribution, so the ELS satisfies WD in RMT.
- [44] A. Auerbach, *Interacting electrons and quantum magnetism*, (Springer Science & Business Media, 1994).
- [45] S. Sachdev, *Quantum Phase transitions*, (2nd edition, Cambridge University Press, 2011).
- [46] Yu Yi-Xiang, Jinwu Ye and Wuming Liu, Quantum chaos and quantum analog of Kolmogorov-Arnold-Moser (KAM) theorem in hybrid Sachdev-Ye-Kitaev models, Preprint.
- [47] F. Brennecke, *et.al*, Nature 450, 268 - 271 (08 Nov 2007);
- [48] Yves Colombe, *et.al*, Nature 450, 272 - 276 (08 Nov 2007).
- [49] A. T. Black, H. W. Chan and V. Vuletic, Phys. Rev. Lett. 91, 203001(2003).
- [50] K. Baumann, *et.al*, Nature 464, 1301-1306 (2010);
- [51] K. Baumann, *et.al*, Phys. Rev. Lett. 107, 140402 (2011).
- [52] A. Wallraff, *et.al*, Nature 431, 162-167 (2004).
- [53] T. Niemczyk, *et.al*, Nature Physics 6,772-776(2010).
- [54] G. Gunter, *et.al*, Nature, Vol 458, 178, 12 March 2009.
- [55] Aji A. Anappara, *et.al*, Phys. Rev. B 79, 201303(R) (2009).
- [56] Reithmaier, J. P, *et.al*, Nature 432, 197-200 (2004); Yoshie, T. *et al*, Nature 432, 200-203 (2004); K. Hennessy, *et al*, Nature 445, 896-899 (22 February 2007).
- [57] D. F. Walls and G. J. Milburn, Quantum Optics, Springer-Verlag, 1994.
- [58] M. O. Scully and M. S. Zubairy, Quantum Optics, Cambridge University press, 1997
- [59] Jinwu Ye, T. Shi and Longhua Jiang, Phys. Rev. Lett. 103, 177401 (2009); T. Shi, Longhua Jiang and Jinwu Ye, Phys. Rev. B 81, 235402 (2010); Jinwu Ye, Fadi Sun, Yi-Xiang Yu and Wuming Liu, Ann. Phys. 329, 51C72 (2013).